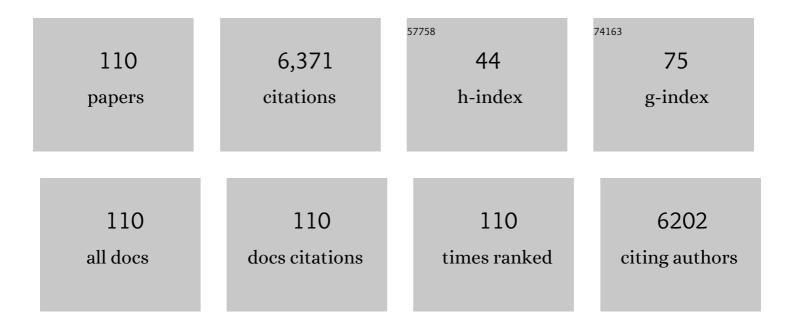
Xiao-Dong Wang

List of Publications by Year in descending order

Source: https://exaly.com/author-pdf/6561155/publications.pdf Version: 2024-02-01



#	Article	IF	CITATIONS
1	Remarkable Performance of Ir ₁ /FeO _{<i>x</i>} Single-Atom Catalyst in Water Gas Shift Reaction. Journal of the American Chemical Society, 2013, 135, 15314-15317.	13.7	811
2	Atomically dispersed nickel as coke-resistant active sites for methane dry reforming. Nature Communications, 2019, 10, 5181.	12.8	398
3	Design of a Highly Active Ir/Fe(OH) _{<i>x</i>} Catalyst: Versatile Application of Ptâ€Group Metals for the Preferential Oxidation of Carbon Monoxide. Angewandte Chemie - International Edition, 2012, 51, 2920-2924.	13.8	183
4	Synthesis of Highâ€Quality Diesel with Furfural and 2â€Methylfuran from Hemicellulose. ChemSusChem, 2012, 5, 1958-1966.	6.8	177
5	Origin of the high activity of Au/FeOx for low-temperature CO oxidation: Direct evidence for a redox mechanism. Journal of Catalysis, 2013, 299, 90-100.	6.2	170
6	Synthesis of renewable high-density fuels using cyclopentanone derived from lignocellulose. Chemical Communications, 2014, 50, 2572.	4.1	143
7	Identifying Size Effects of Pt as Single Atoms and Nanoparticles Supported on FeO _{<i>x</i>} for the Water-Gas Shift Reaction. ACS Catalysis, 2018, 8, 859-868.	11.2	140
8	Aqueous phase hydrogenation of levulinic acid to 1,4-pentanediol. Chemical Communications, 2014, 50, 1414.	4.1	136
9	Catalytically Active Rh Subâ€Nanoclusters on TiO ₂ for CO Oxidation at Cryogenic Temperatures. Angewandte Chemie - International Edition, 2016, 55, 2820-2824.	13.8	127
10	Synthesis of renewable diesel with hydroxyacetone and 2-methyl-furan. Chemical Communications, 2013, 49, 5727.	4.1	116
11	Controlling CO ₂ Hydrogenation Selectivity by Metal‣upported Electron Transfer. Angewandte Chemie - International Edition, 2020, 59, 19983-19989.	13.8	114
12	Little do more: a highly effective Pt ₁ /FeO _x single-atom catalyst for the reduction of NO by H ₂ . Chemical Communications, 2015, 51, 7911-7914.	4.1	107
13	Dual Metal Active Sites in an Ir ₁ /FeO _{<i>x</i>} Singleâ€Atom Catalyst: A Redox Mechanism for the Waterâ€Gas Shift Reaction. Angewandte Chemie - International Edition, 2020, 59, 12868-12875.	13.8	102
14	Recent progress in CO oxidation over Pt-group-metal catalysts at low temperatures. Chinese Journal of Catalysis, 2016, 37, 1805-1813.	14.0	97
15	"lr-in-ceria― A highly selective catalyst for preferential CO oxidation. Journal of Catalysis, 2008, 255, 144-152.	6.2	91
16	Synergy of the catalytic activation on Ni and the CeO ₂ –TiO ₂ /Ce ₂ Ti ₂ O ₇ stoichiometric redox cycle for dramatically enhanced solar fuel production. Energy and Environmental Science, 2019, 12, 767-779.	30.8	90
17	Synthesis of renewable diesel with the 2-methylfuran, butanal and acetone derived from lignocellulose. Bioresource Technology, 2013, 134, 66-72.	9.6	88
18	Coordinatively Unsaturated Al ³⁺ Sites Anchored Subnanometric Ruthenium Catalyst for Hydrogenation of Aromatics. ACS Catalysis, 2017, 7, 5987-5991.	11.2	88

#	Article	IF	CITATIONS
19	Synthesis of Diesel and Jet Fuel Range Alkanes with Furfural and Angelica Lactone. ACS Catalysis, 2017, 7, 5880-5886.	11.2	85
20	Unique role of Mössbauer spectroscopy in assessing structural features of heterogeneous catalysts. Applied Catalysis B: Environmental, 2018, 224, 518-532.	20.2	83
21	Synthesis of renewable diesel range alkanes by hydrodeoxygenation of furans over Ni/Hβ under mild conditions. Green Chemistry, 2014, 16, 594-599.	9.0	79
22	Making JPâ€10 Superfuel Affordable with a Lignocellulosic Platform Compound. Angewandte Chemie - International Edition, 2019, 58, 12154-12158.	13.8	78
23	Enhanced performance of Rh ₁ /TiO ₂ catalyst without methanation in waterâ€gas shift reaction. AICHE Journal, 2017, 63, 2081-2088.	3.6	74
24	In Situ Calorimetric Study: Structural Effects on Adsorption and Catalytic Performances for CO Oxidation over Ir-in-CeO ₂ and Ir-on-CeO ₂ Catalysts. Journal of Physical Chemistry C, 2011, 115, 16509-16517.	3.1	73
25	Lignosulfonate-based acidic resin for the synthesis of renewable diesel and jet fuel range alkanes with 2-methylfuran and furfural. Green Chemistry, 2015, 17, 3644-3652.	9.0	73
26	Enhanced performance of boron nitride catalysts with induction period for the oxidative dehydrogenation of ethane to ethylene. Journal of Catalysis, 2018, 365, 14-23.	6.2	73
27	Remarkable effects of hydroxyl species on low-temperature CO (preferential) oxidation over Ir/Fe(OH) x catalyst. Journal of Catalysis, 2014, 319, 142-149.	6.2	71
28	FeO _x supported singleâ€atom Pd bifunctional catalyst for water gas shift reaction. AICHE Journal, 2017, 63, 4022-4031.	3.6	70
29	Hydroformylation of Olefins by a Rhodium Singleâ€Atom Catalyst with Activity Comparable to RhCl(PPh ₃) ₃ . Angewandte Chemie, 2016, 128, 16288-16292.	2.0	67
30	High-Efficiency Water Gas Shift Reaction Catalysis on α-MoC Promoted by Single-Atom Ir Species. ACS Catalysis, 2021, 11, 5942-5950.	11.2	65
31	Synthesis of gasoline and jet fuel range cycloalkanes and aromatics from poly(ethylene terephthalate) waste. Green Chemistry, 2019, 21, 2709-2719.	9.0	61
32	A molten carbonate shell modified perovskite redox catalyst for anaerobic oxidative dehydrogenation of ethane. Science Advances, 2020, 6, eaaz9339.	10.3	61
33	Synthesis of Renewable High-Density Fuel with Cyclopentanone Derived from Hemicellulose. ACS Sustainable Chemistry and Engineering, 2017, 5, 1812-1817.	6.7	60
34	Improving Syngas Selectivity of Fe ₂ O ₃ /Al ₂ O ₃ with Yttrium Modification in Chemical Looping Methane Conversion. ACS Catalysis, 2019, 9, 8373-8382.	11.2	59
35	In situ encapsulation of iron(0) for solar thermochemical syngas production over iron-based perovskite material. Communications Chemistry, 2018, 1, .	4.5	55
36	Identification of Active Sites on High-Performance Pt/Al ₂ O ₃ Catalyst for Cryogenic CO Oxidation. ACS Catalysis, 2020, 10, 8815-8824.	11.2	54

#	Article	IF	CITATIONS
37	Stabilization mechanism and crystallographic sites of Ru in Fe-promoted barium hexaaluminate under high-temperature condition for N2O decomposition. Applied Catalysis B: Environmental, 2013, 129, 382-393.	20.2	51
38	Highly active subnano Rh/Fe(OH) catalyst for preferential oxidation of CO in H2-rich stream. Applied Catalysis B: Environmental, 2016, 184, 299-308.	20.2	51
39	Bimetallic BaFe2MAl9O19 (M = Mn, Ni, and Co) hexaaluminates as oxygen carriers for chemical looping dry reforming of methane. Applied Energy, 2020, 258, 114070.	10.1	51
40	Effect of large cations (La3+ and Ba2+) on the catalytic performance of Mn-substituted hexaaluminates for N2O decomposition. Applied Catalysis B: Environmental, 2009, 92, 437-444.	20.2	50
41	Synthesis of High-Density Aviation Fuel with Cyclopentanol. ACS Sustainable Chemistry and Engineering, 2016, 4, 6160-6166.	6.7	50
42	Sn promoted BaFeO3â^' catalysts for N2O decomposition: Optimization of Fe active centers. Journal of Catalysis, 2017, 347, 9-20.	6.2	50
43	Identifying the Role of A-Site Cations in Modulating Oxygen Capacity of Iron-Based Perovskite for Enhanced Chemical Looping Methane-to-Syngas Conversion. ACS Catalysis, 2020, 10, 9420-9430.	11.2	48
44	Unravelling platinum nanoclusters as active sites to lower the catalyst loading for formaldehyde oxidation. Communications Chemistry, 2019, 2, .	4.5	47
45	Laâ€hexaaluminate for synthesis gas generation by Chemical Looping Partial Oxidation of Methane Using CO ₂ as Sole Oxidant. AICHE Journal, 2018, 64, 550-563.	3.6	46
46	Effect of Regeneration Period on the Selectivity of Synthesis Gas of Ba-Hexaaluminates in Chemical Looping Partial Oxidation of Methane. ACS Catalysis, 2019, 9, 722-731.	11.2	46
47	Identification of the chemical state of Fe in barium hexaaluminate using Rietveld refinement and 57Fe Mössbauer spectroscopy. Journal of Catalysis, 2011, 283, 149-160.	6.2	42
48	Synthesis of jet fuel range cycloalkanes with diacetone alcohol from lignocellulose. Green Chemistry, 2016, 18, 5751-5755.	9.0	41
49	More active Ir subnanometer clusters than singleâ€atoms for catalytic oxidation of CO at low temperature. AICHE Journal, 2017, 63, 4003-4012.	3.6	41
50	Local structure of Pt species dictates remarkable performance on Pt/Al2O3 for preferential oxidation of CO in H2. Applied Catalysis B: Environmental, 2021, 282, 119588.	20.2	41
51	Highly Active and Anticoke Ni/CeO ₂ with Ultralow Ni Loading in Chemical Looping Dry Reforming via the Strong Metal–Support Interaction. ACS Sustainable Chemistry and Engineering, 2021, 9, 17276-17288.	6.7	41
52	Industrially scalable and cost-effective synthesis of 1,3-cyclopentanediol with furfuryl alcohol from lignocellulose. Green Chemistry, 2016, 18, 3607-3613.	9.0	37
53	Highly efficient synthesis of 5-hydroxymethylfurfural with carbohydrates over renewable cyclopentanone-based acidic resin. Green Chemistry, 2017, 19, 1855-1860.	9.0	35
54	A novel CeO ₂ – <i>x</i> SnO ₂ /Ce ₂ Sn ₂ O ₇ pyrochlore cycle for enhanced solar thermochemical water splitting. AICHE Journal, 2017, 63, 3450-3462.	3.6	34

#	Article	IF	CITATIONS
55	Microstructure and reactivity evolution of La Fe Al oxygen carrier for syngas production via chemical looping CH4CO2 reforming. International Journal of Hydrogen Energy, 2017, 42, 30509-30524.	7.1	34
56	Improving the selectivity of Ni-Al mixed oxides with isolated oxygen species for oxidative dehydrogenation of ethane with nitrous oxide. Journal of Catalysis, 2019, 377, 438-448.	6.2	33
57	Synthesis of renewable diesel with 2-methylfuran and angelica lactone derived from carbohydrates. Green Chemistry, 2016, 18, 1218-1223.	9.0	32
58	Recent Advances of Oxygen Carriers for Chemical Looping Reforming of Methane. ChemCatChem, 2021, 13, 1615-1637.	3.7	32
59	A palladium single-atom catalyst toward efficient activation of molecular oxygen for cinnamyl alcohol oxidation. Chinese Journal of Catalysis, 2020, 41, 1812-1817.	14.0	31
60	IrFeOx/SiO2—A highly active catalyst for preferential CO oxidation in H2. International Journal of Hydrogen Energy, 2010, 35, 3065-3071.	7.1	30
61	Dehydration of Carbohydrates to 5-Hydroxymethylfurfural over Lignosulfonate-Based Acidic Resin. ACS Sustainable Chemistry and Engineering, 2018, 6, 5645-5652.	6.7	30
62	Synthesis of jet fuel range high-density polycycloalkanes with polycarbonate waste. Green Chemistry, 2019, 21, 3789-3795.	9.0	30
63	Near 100% ethene selectivity achieved by tailoring dual active sites to isolate dehydrogenation and oxidation. Nature Communications, 2021, 12, 5447.	12.8	30
64	Feâ€substituted Baâ€hexaaluminates oxygen carrier for carbon dioxide capture by chemical looping combustion of methane. AICHE Journal, 2016, 62, 792-801.	3.6	29
65	Synthesis of Renewable C ₈ –C ₁₀ Alkanes with Angelica Lactone and Furfural from Carbohydrates. ACS Sustainable Chemistry and Engineering, 2018, 6, 6126-6134.	6.7	29
66	Synthesis of high-density aviation fuels with methyl benzaldehyde and cyclohexanone. Green Chemistry, 2018, 20, 3753-3760.	9.0	29
67	Microkinetic Study of CO Oxidation and PROX on Irâ^'Fe Catalyst. Industrial & Engineering Chemistry Research, 2011, 50, 758-766.	3.7	27
68	Metal modified hexaaluminates for syngas generation and CO2 utilization via chemical looping. International Journal of Hydrogen Energy, 2019, 44, 10218-10231.	7.1	27
69	Promoted methane conversion to syngas over Fe-based garnets via chemical looping. Applied Catalysis B: Environmental, 2020, 278, 119305.	20.2	27
70	Oxygen Activity Tuning via FeO ₆ Octahedral Tilting in Perovskite Ferrites for Chemical Looping Dry Reforming of Methane. ACS Catalysis, 2022, 12, 7326-7335.	11.2	27
71	Microcalorimetric studies of the iridium catalyst for hydrazine decomposition reaction. Thermochimica Acta, 2005, 434, 119-124.	2.7	26
72	Sulfate-Modified NiAl Mixed Oxides as Effective C–H Bond-Breaking Agents for the Sole Production of Ethylene from Ethane. ACS Catalysis, 2020, 10, 7619-7629.	11.2	26

#	Article	IF	CITATIONS
73	Evolution of Fe Crystallographic Sites from Barium Hexaaluminate to Hexaferrite. Journal of Physical Chemistry C, 2012, 116, 671-680.	3.1	25
74	A two-step synthesis of Fe-substituted hexaaluminates with enhanced surface area and activity in methane catalytic combustion. Catalysis Science and Technology, 2016, 6, 4962-4969.	4.1	25
75	High performance of laâ€promoted Fe ₂ O ₃ /αâ€Al ₂ O ₃ oxygen carrier for chemical looping combustion. AICHE Journal, 2017, 63, 2827-2838.	3.6	25
76	Silica Modified Alumina As Supports of Fe ₂ O ₃ with High Performance in Chemical Looping Combustion of Methane. ACS Sustainable Chemistry and Engineering, 2018, 6, 12884-12892.	6.7	25
77	Reactivity of Methanol Steam Reforming on ZnPd Intermetallic Catalyst: Understanding from Microcalorimetric and FT-IR Studies. Journal of Physical Chemistry C, 2018, 122, 12395-12403.	3.1	25
78	Fe-substituted Ba-hexaaluminate with enhanced oxygen mobility for CO2 capture by chemical looping combustion of methane. Journal of Energy Chemistry, 2019, 29, 50-57.	12.9	25
79	Anti-coke BaFe _{1–<i>x</i>} Sn _{<i>x</i>} O _{3â^î^} Oxygen Carriers for Enhanced Syngas Production via Chemical Looping Partial Oxidation of Methane. Energy & Fuels, 2020, 34, 6991-6998.	5.1	24
80	Catalytic decomposition of propellant N ₂ O Over Ir/Al ₂ O ₃ catalyst. AICHE Journal, 2016, 62, 3973-3981.	3.6	23
81	Synthesis of Decaline-Type Thermal-Stable Jet Fuel Additives with Cycloketones. ACS Sustainable Chemistry and Engineering, 2019, 7, 17354-17361.	6.7	21
82	α-MoC Supported Noble Metal Catalysts for Water–Gas Shift Reaction: Single-Atom Promoter or Single-Atom Player. Journal of Physical Chemistry Letters, 2021, 12, 11415-11421.	4.6	21
83	Defect-Rich TiO ₂ <i>In Situ</i> Evolved from MXene for the Enhanced Oxidative Dehydrogenation of Ethane to Ethylene. ACS Catalysis, 2021, 11, 15223-15233.	11.2	20
84	Relationship between adsorption properties of Pt–Cu/SiO2 catalysts and their catalytic performance for selective hydrodechlorination of 1,2-dichloroethane to ethylene. Thermochimica Acta, 2009, 494, 99-103.	2.7	19
85	Effect of magnesium substitution into Fe-based La-hexaaluminates on the activity for CH4 catalytic combustion. Catalysis Science and Technology, 2016, 6, 7860-7867.	4.1	19
86	Exceptional Antisintering Gold Nanocatalyst for Diesel Exhaust Oxidation. Nano Letters, 2018, 18, 6489-6493.	9.1	19
87	Synthesis of jet fuel additive with cyclopentanone. Journal of Energy Chemistry, 2019, 29, 23-30.	12.9	19
88	Dual Metal Active Sites in an Ir ₁ /FeO _{<i>x</i>} Singleâ€Atom Catalyst: A Redox Mechanism for the Waterâ€Gas Shift Reaction. Angewandte Chemie, 2020, 132, 12968-12975.	2.0	19
89	Effect of calcination temperature on the performance of hexaaluminate supported CeO2 for chemical looping dry reforming. Fuel Processing Technology, 2021, 218, 106873.	7.2	19
90	Hydrogenated TiO2 supported Ru for selective methanation of CO in practical conditions. Applied Catalysis B: Environmental, 2021, 298, 120597.	20.2	19

#	Article	IF	CITATIONS
91	Direct synthesis of a high-density aviation fuel using a polycarbonate. Green Chemistry, 2021, 23, 912-919.	9.0	19
92	Widening Temperature Window for CO Preferential Oxidation in H ₂ by Ir Nanoparticles Interaction with Framework Fe of Hexaaluminate. ACS Catalysis, 2021, 11, 5709-5717.	11.2	18
93	Selective catalytic oxidation of ammonia to nitric oxide via chemical looping. Nature Communications, 2022, 13, 718.	12.8	18
94	Thermodynamic analysis of chemical looping coupling process for coproducing syngas and hydrogen with in situ CO2 utilization. Energy Conversion and Management, 2021, 231, 113845.	9.2	17
95	Exerting the structural advantages of Ir-in-CeO2 and Ir-on-CeO2 to widen the operating temperature window for preferential CO oxidation. Chemical Engineering Journal, 2011, 168, 822-826.	12.7	16
96	Solid Acid-Catalyzed Dehydration of Pinacol Derivatives in Ionic Liquid: Simple and Efficient Access to Branched 1,3-Dienes. ACS Catalysis, 2017, 7, 2576-2582.	11.2	16
97	Low-temperature conversion of methane to oxygenates by supported metal catalysts: From nanoparticles to single atoms. Chinese Journal of Chemical Engineering, 2021, 38, 18-29.	3.5	16
98	Direct synthesis of a jet fuel range dicycloalkane by the aqueous phase hydrodeoxygenation of polycarbonate. Green Chemistry, 2021, 23, 3693-3699.	9.0	16
99	Intensified solar thermochemical CO2 splitting over iron-based redox materials via perovskite-mediated dealloying-exsolution cycles. Chinese Journal of Catalysis, 2021, 42, 2049-2058.	14.0	13
100	Noble-metal based single-atom catalysts for the water-gas shift reaction. Chemical Communications, 2021, 58, 208-222.	4.1	13
101	Adsorption/reaction energetics measured by microcalorimetry and correlated with reactivity on supported catalysts: A review. Chinese Journal of Catalysis, 2016, 37, 2039-2052.	14.0	10
102	A novel carbon cycle process assisted by Ni/La2O3 catalyst for enhanced thermochemical CO2 splitting. Journal of Energy Chemistry, 2021, 61, 297-303.	12.9	10
103	Synthesis of jet fuel range polycyclic alkanes and aromatics from furfuryl alcohol and isoprene. Green Chemistry, 2022, 24, 3130-3136.	9.0	10
104	Controlling CO 2 Hydrogenation Selectivity by Metalâ€&upported Electron Transfer. Angewandte Chemie, 2020, 132, 20158-20164.	2.0	8
105	Influence of the encapsulation degree of FeO active sites on performance of garnets for chemical looping partial oxidation of CH4. Applied Catalysis B: Environmental, 2022, 312, 121421.	20.2	8
106	Versatile application of wet-oxidation for ambient CO abatement over Fe(OH) supported subnanometer platinum group metal catalysts. Chinese Journal of Catalysis, 2020, 41, 613-621.	14.0	6
107	Breaking the Stoichiometric Limit in Oxygen-Carrying Capacity of Fe-Based Oxygen Carriers for Chemical Looping Combustion using the Mg-Fe-O Solid Solution System. ACS Sustainable Chemistry and Engineering, 2022, 10, 7242-7252.	6.7	6
108	Synthesis of renewable alkylated decalins with <i>p</i> -quinone and 2-methyl-2,4-pentanediol. Sustainable Energy and Fuels, 2022, 6, 834-840.	4.9	5

#	Article	IF	CITATIONS
109	Synthesis of jet fuel and diesel range cycloalkanes with 2-methylfuran and benzaldehyde. Sustainable Energy and Fuels, 2022, 6, 1156-1163.	4.9	4
110	Synthesis of renewable alkylated naphthalenes with benzaldehyde and angelica lactone. Green Chemistry, 2021, 23, 5474-5480.	9.0	0